

## On-Flow Ligand Screening Assay Based on Immobilized Nucleoside Diphosphate Kinase B from *Homo sapiens*

Juliana M. Lima,<sup>a</sup> Claudia Seidl,<sup>a</sup> Elise M. F. Cunha,<sup>a,b</sup> Arthur H. C. Oliveira<sup>a</sup> and Carmen L. Cardoso<sup>✉\*,a</sup>

<sup>a</sup>Departamento de Química, Grupo de Cromatografia de Bioafinidade e Produtos Naturais, Faculdade de Filosofia, Ciências e Letras de Ribeirão Preto, Universidade de São Paulo, 14040-900 Ribeirão Preto-SP, Brazil

<sup>b</sup>Instituto Federal de Educação, Ciência e Tecnologia de Rondônia, Campus Ji-Paraná, 76900-000 Ji-Paraná-RO, Brazil

We describe an on-flow zonal affinity-based chromatography assay to screen ligands for the nucleoside diphosphate kinase B enzyme (NME2) from *Homo sapiens*. For the first time, we have covalently immobilized NME2 on the surface of an open fused silica capillary reactor (NME2-ICER) and placed the reactor before the analytical column, which resulted in a two-dimensional liquid chromatography-based system. We evaluated the pH effect on immobilized NME2 activity and carried out steady-state kinetic studies to compare free and immobilized NME2. Steady-state kinetic studies with the substrates adenosine 5'-triphosphate di(tris) salt dihydrate (ATP) and guanosine 5'-diphosphate sodium salt (GDP) resulted in apparent Michaelis-Menten constant values of 1136 and 713 mmol L<sup>-1</sup>, respectively. The ping-pong catalysis mechanism and substrate specificity were preserved after NME2 immobilization. By employing a reference inhibitor, (-)-epicatechin gallate (ECG), we verified the potential application of this method in NME2 ligand screening and NME2 inhibitor identification. The half maximum inhibitory concentration (IC<sub>50</sub>) for ECG was 161.3 ± 1.0 μmol L<sup>-1</sup>.

**Keywords:** two-dimensional chromatography, kinase inhibitors assay, tight-binding, ping-pong mechanism

### Introduction

The success of a drug-discovery project depends upon having not only a well-characterized target and a good compound library, but also efficient and appropriate screening technologies to identify valuable chemical starting points.<sup>1</sup>

Nucleoside diphosphate kinase (NDPK; EC 2.7.4.6) is an ubiquitous enzyme that catalyzes γ-phosphoryl transfer from a triphosphate nucleotide (NTP) to a diphosphate nucleotide (NDP), including 2'-desoxynucleoside.<sup>2</sup> This transfer occurs through a ping-pong mechanism that involves a covalent intermediate in which the enzyme is transiently phosphorylated at a histidine residue.<sup>2,3</sup>

In humans, the gene family NDPK consists of ten members (designated NME1-9 and RP2; non-metastatic).<sup>4,5</sup> NME1 (nucleoside diphosphate kinase A) and NME2 (nucleoside diphosphate kinase B) are the most abundant

subunits in human cells and have been extensively studied.<sup>4</sup> Despite the structural similarity between these subunits, protein NME1 suppresses metastasis,<sup>6</sup> whereas NME2 seems to be inversely correlated with metastatic potential.<sup>7-9</sup>

Albeit controversial, *in vitro* and *in vivo* studies have also shown higher NME2 protein expression in several kinds of human cancers such as hepatocellular carcinoma, breast cancer, colorectal cancer, pancreatic cancer, lung cancer, endometrial cancer, and liver cell tumor.<sup>7,9-13</sup> More recently, NME2 inhibition by stauprimide has been demonstrated to down-regulate MYC transcription with consequent tumor growth inhibition in an animal model.<sup>14</sup> Additionally, *in vivo* studies on NME2 blockade impact have revealed decreased tumor growth and metastasis in breast cancer.<sup>15</sup> Furthermore, NME2 knockdown has been shown to reduce cell survival and to increase cell apoptosis in colorectal cancer cells.<sup>16</sup> Thus, finding a small molecule that can inhibit NME2 activity may aid cancer therapy.

NDPK activity is usually measured by means of a coupled pyruvate kinase/lactate dehydrogenase

\*e-mail: ccardoso@ffclrp.usp.br

spectrophotometric enzymatic assay. This indirect assay measures nicotinamide adenine dinucleotide (NADH) oxidation coupled to NTP hydrolysis<sup>17</sup> and can lead to false positive and/or false negative results because it is based on indirect NDPK activity measurement.

To overcome these drawbacks, developing innovative and efficient direct assays that can recognize and characterize NME2 inhibitors is extremely relevant for the drug discovery process. Immobilized capillary enzyme reactors (ICERs) have already proven to be an efficient tool to develop completely automated on-flow immobilized enzyme-based screening systems, to carry out standard enzyme kinetic studies, and to characterize ligands for numerous therapeutic enzymes, like cholinesterases,<sup>18-20</sup>  $\beta$ -secretase (BACE1),<sup>21</sup> gelatinase,<sup>22</sup> and glucose-6-phosphate dehydrogenase.<sup>23</sup> These immobilized reactor-based systems have already been successfully used to study enzyme kinetics and to investigate enzyme inhibition through application of both zonal<sup>19,24-28</sup> and frontal<sup>25,26,29-31</sup> affinity-based strategies.

Here, we describe a two-dimensional on-flow zonal affinity-based chromatography assay for NME2 coupled to an ion-pair reversed-phase high-performance liquid chromatography system (ion-pair RP-HPLC). For the first time, we report on successful covalent NME2 immobilization on open tubular silica capillary (named NME2-ICER). We have evaluated possible changes in NME2 structural conformation and/or substrate binding sites after NME2 immobilization by verifying the pH effect on enzymatic activity with the aid of steady-state kinetic studies for free and immobilized NME2. To validate the applicability of the assay to screen ligands for NME2, we have employed a well-known phosphotransferase inhibitor, (-)-epicatechin gallate (ECG), and determined the half maximum inhibitory concentration (IC<sub>50</sub>).

## Experimental

### Materials

Adenosine 5'-triphosphate di(tris) salt dihydrate (ATP), guanosine 5'-diphosphate sodium salt (GDP), adenosine-5'-diphosphate sodium salt (ADP), and guanosine-5'-triphosphate tris salt (GTP) were purchased from Sigma-Aldrich (St. Louis, USA).

ECG was provided by Prof Dr Anita J. Marsaioli of the University of Campinas (UNICAMP, Campinas, Brazil). Buffer constituents and all reagents that were used to immobilize, to express, and to purify the enzyme were supplied by Sigma-Aldrich (St. Louis, USA), Acros (Geel, Belgium), J.T. Baker (Xalostoc, Mexico), Merck (Darmstadt, Germany), Qiagen (Hilden, Germany), and

GE Healthcare (Little Chalfont, United Kingdom). The standard coated open silica capillary tubing (0.375 mm o.d.  $\times$  0.100 mm i.d., code: TPS100375) was obtained from Polymicro (Phoenix, USA). All solutions were prepared with ultrapure water purified in a Millipore Progard<sup>®</sup> 2 system (São Paulo, Brazil). All buffer solutions were filtered on cellulose nitrate membranes (0.45  $\mu$ m) provided by Phenomenex<sup>®</sup> (Torrance, USA). All chemicals and solvents used in the experiments had analytical or HPLC grade and were used without further purification.

### Instrumentation

The two-dimensional on-flow zonal affinity-based chromatography assay was set up as illustrated in Figure 1 (system 1). The first dimension, where the on-flow enzyme reaction took place, consisted of a Shimadzu Prominence LC20 AD binary pump, a Shimadzu Prominence SIL-20A auto-sampler (Kyoto, Japan), and NME2-ICER. The second dimension, where the nucleotides were separated, comprised a Shimadzu Prominence LC20 AD binary pump (Kyoto, Japan) with incorporated low-pressure gradient valve (LC-20AD/20AT), a two-position and three-way electronically controlled VICI Cheminert switching valve (model EHMA from Valco, Houston, USA), an octadecyl column (Eclipse XDB Agilent<sup>®</sup>, 5  $\mu$ m, 100 Å, 150  $\times$  0.46 mm i.d., Santa Clara, USA), and a Shimadzu Prominence SPD-M20A diode array detector (Kyoto, Japan). The two-dimensional system was controlled by a CBM-20A controller, and data were acquired with LC Solution software (version 2.1).

To measure the free NME2 activity, a simplified version of system 1 was employed. This version (system 2) consisted of a Shimadzu Prominence SIL-20A auto-sampler (Kyoto, Japan), a Shimadzu Prominence LC20 AD binary pump (Kyoto, Japan), an octadecyl column (Eclipse XDB Agilent<sup>®</sup>, 5  $\mu$ m, 100 Å, 150  $\times$  0.46 mm i.d., Santa Clara, USA), and a Shimadzu Prominence SPD-M20A diode array detector (Kyoto, Japan). System 2 was also controlled by a CBM-20A controller.

### Protein expression and purification

cDNA encoding NME2 was cloned into vector pET28a (Novagen, Madison, USA) with an N-terminal histidine tag. Recombinant NME2 was overexpressed in *E. coli* strain BL21 (DE3) as reported for *Leishmania major* nucleoside diphosphate kinase B (*LmNDKb*) in reference.<sup>32</sup> Briefly, recombinant NME2 was induced with 1.0 mmol L<sup>-1</sup> isopropyl- $\beta$ -D-thiogalactopyranoside (IPTG) for 5 h, and the enzyme was purified by affinity chromatography

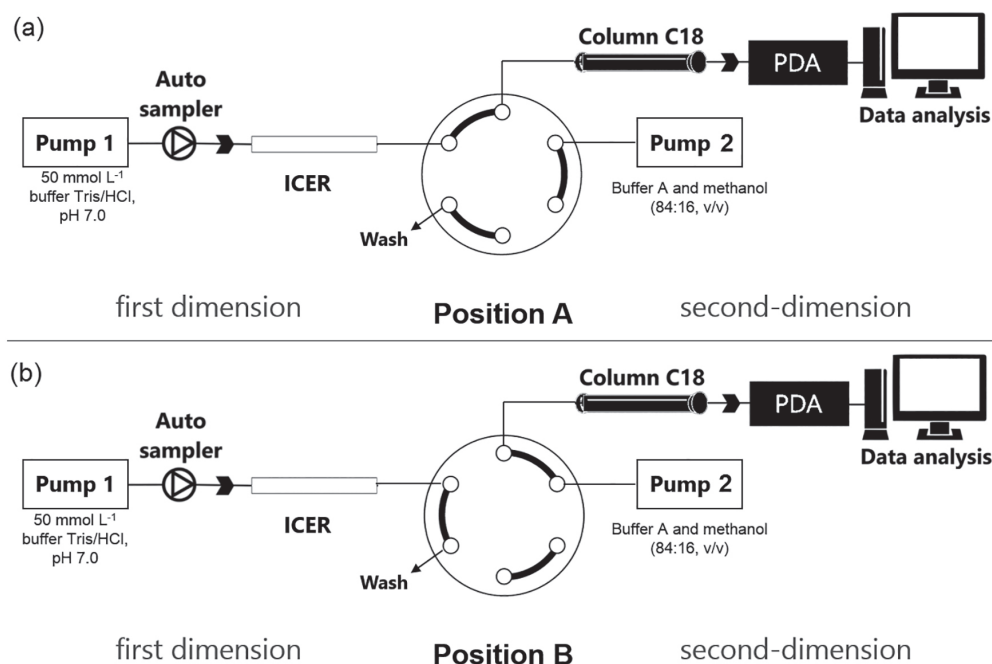


**Figure 1.** Schematic diagram of the two-dimensional on-flow zonal affinity-based chromatography assay. (a) Initially, the valve remains in position A, and the enzymatic reaction occurs in NME2-ICER; (b) after that, the valve changes positions, and the products (ADP and GTP) and unreacted substrates (ATP and GDP) are separated by ion-pair RP-HPLC in the second dimension and detected at 254 nm.

with the aid of a  $\text{Ni}^{2+}$  chelating resin. Protein expression and purity were verified by 15% SDS-PAGE. Next, the concentration of the fractions with the highest purity were estimated by the Bradford method;<sup>33</sup> bovine serum albumin was used as standard.

#### NME2-ICER preparation

Recombinant NME2 was covalently immobilized on the internal surface of a standard coated open silica capillary tubing (100 cm  $\times$  0.375 mm  $\times$  0.1 mm i.d.) as previously described and optimized for *L. major* NDKb,<sup>28</sup> with few modifications. Briefly, 500  $\mu\text{L}$  of recombinant NME2 solution (250 ng  $\mu\text{L}^{-1}$  in 150 mmol  $\text{L}^{-1}$  imidazole buffer containing 300 mmol  $\text{L}^{-1}$  NaCl and 50 mmol  $\text{L}^{-1}$   $\text{NaH}_2\text{PO}_4$ ) was infused into the capillary at 130  $\mu\text{L min}^{-1}$ . NME2 solution was collected, and the step was repeated three times. The 100 cm long immobilized capillary enzyme reactor was divided, which generated three 30 cm long reactors. The effect of the NME2 solution pH on the immobilization procedure was evaluated by using NME2 solutions with pH 8 and 10.

A syringe pump model 11 Plus advanced single from Harvard Apparatus (Holliston, USA) was employed to infuse all the solutions during the immobilization procedure. While NME2-ICER was not being used, it was stored at 4  $^\circ\text{C}$  with both tips immersed in 50 mmol  $\text{L}^{-1}$  Tris/HCl buffer, pH 7.0.

To assess immobilization procedure repeatability, the initial activities of six freshly prepared NME2-ICERs from two independent experiments were determined.

NME2-ICER stability was evaluated by periodically monitoring NME2 activity for 320 days after immobilization.

NME2-ICER activities were measured by injecting the substrates ATP and GDP (both at 1.0 mmol  $\text{L}^{-1}$  in 50 mmol  $\text{L}^{-1}$  Tris/HCl buffer, pH 7.0, containing 5 mmol  $\text{L}^{-1}$   $\text{MgCl}_2$  and 100 mmol  $\text{L}^{-1}$  NaCl) into the two-dimensional on-flow zonal affinity-based chromatography system (see “Two-dimensional on-flow zonal affinity-based chromatography assay” sub-section).

Immobilization efficiency was evaluated in terms of stability and activity recovery and expressed as a percentage, according to equation 1:

$$\text{Activity recovery(\%)} = \frac{\text{Immobilized NME2 activity}}{\text{Free NME2 activity}} \times 100 \quad (1)$$

#### Free NME2 activity assay

NME2 activity in solution was investigated by using system 2 (free NME2 activity assay) by directly quantifying ADP production. Conditions for this enzymatic assay were designed as previously described,<sup>28,32</sup> with minimal modifications. Briefly, the reaction mixture consisted of 100  $\mu\text{L}$  of a solution containing the substrates ATP and GDP (both at 1 mmol  $\text{L}^{-1}$  in 50 mmol  $\text{L}^{-1}$  Tris/HCl buffer,

pH 7.0, containing 5 mmol L<sup>-1</sup> MgCl<sub>2</sub> and 100 mmol L<sup>-1</sup> NaCl) and 250 ng μL<sup>-1</sup> NME2. The reaction mixture was incubated at 37 °C for 10 min and was stopped by heating to 80 °C. An aliquot (20 μL) of this mixture was directly injected into system 2. The products (ADP and GTP) and unreacted substrates (ATP and GDP) were separated by ion-pair RP-HPLC (see “Two-dimensional on-flow zonal affinity-based chromatography assay” sub-section).

#### Two-dimensional on-flow zonal affinity-based chromatography assay

Analyses were performed by using system 1, described above. The mobile phase employed in the first dimension was 50 mmol L<sup>-1</sup> Tris/HCl buffer, pH 7.0, which was infused at 100 μL min<sup>-1</sup> by pump 1. The nucleotide mixture was completely transferred to the second dimension by means of a three-way/two-position switching valve (Figure 1a). Then, the nucleotides were separated in an octadecyl ion-pair RP-HPLC column (Figure 1b). The second-dimension binary mobile phase was infused by pump 2 at 1.0 mL min<sup>-1</sup> and was composed of 84:16 (v/v) of buffer A (50 mmol L<sup>-1</sup> potassium phosphate monobasic, pH 4.7, 80 mmol L<sup>-1</sup> ammonium chloride, and 3.0 mmol L<sup>-1</sup> tetrabutylammonium hydrogensulfate) and B (methanol). All analyses were performed at room temperature (21 °C), and 20 μL of the samples were injected. The UV detector absorption wavelength was set at 254 nm.

#### Optimization

NME2-ICER activity was evaluated by using different flow rates ranging from 30 to 250 μL min<sup>-1</sup> and different transfer times ranging from 1 to 6 min.

The pH effect on the free and immobilized enzyme activities was evaluated by determining these activities at pH values ranging from 4.0 to 9.0. The activities were evaluated by using 50 mmol L<sup>-1</sup> citrate-phosphate buffer (pH 4.0-7.0, with 0.5-unit intervals) and 50 mmol L<sup>-1</sup> Tris buffer (pH 7.0-9.0).

#### Method qualification

Both the two-dimensional on-flow zonal affinity-based chromatography assay and the free NME2 activity assay were qualified according to Food and Drug Administration (FDA) bioanalytical guidelines.<sup>34</sup> Qualifications included evaluation of linearity, selectivity, limits of detection (LOD), and limits of quantification (LOQ).

Linearity was determined by means of the ADP standard external calibration curves. To this end, different ADP stock solutions at concentrations ranging from 50 to 1500 μmol L<sup>-1</sup> were prepared. An aliquot (10 μL) of

each ADP stock solution was further diluted to a final volume of 100 μL in 50 mmol L<sup>-1</sup> Tris/HCl buffer, pH 7.0, containing 5 mmol L<sup>-1</sup> MgCl<sub>2</sub> and 100 mmol L<sup>-1</sup> NaCl. Aliquots (20 μL) were injected into system 2 in triplicate. For the two-dimensional on-flow zonal affinity-based chromatography assay, an empty capillary was employed. Each respective calibration curve was obtained by plotting the ADP peak area *versus* the injected ADP concentration. To assess method selectivity, chromatograms of the blank runs without the target analytes were examined. The precision determined at each concentration level should not exceed 15% of the coefficient of variation (CV) except for the LOQ, where it should not exceed 20% of the CV.<sup>34</sup> The acceptance criteria for the LOQ were that the accuracy of three samples should be under 20% variability, while the LOD was defined by considering a signal-to-noise ratio of 3.

#### Organic solvent effect on NME2-ICER activity

NME2-ICER activity was also monitored in the presence of different organic solvents, including acetonitrile, dimethyl sulfoxide (DMSO), ethanol, and methanol. Reaction mixtures were prepared by mixing 10 μL of GDP stock solution (10 mmol L<sup>-1</sup>) and 10 μL of ATP stock solution (10 mmol L<sup>-1</sup>) with each solvent to obtain a final concentration of 25 and 50% (v/v). Each reaction mixture (20 μL) was injected into NME2-ICER by using two-dimensional on-flow zonal affinity-based chromatography assay, in triplicate. The separation of two peaks is usually described in terms of their resolution,  $R_s = (\text{difference in retention times})/(\text{average peak width})$ .<sup>35</sup> Thus, the ADP peak area at 254 nm in the presence of each organic solvent was measured and compared to the control (without organic solvent) in terms of  $R_s$  and relative activity.

#### NME2 steady-state kinetics

To generate Michaelis-Menten and Lineweaver-Burk plots, the final concentration of the phosphate donor substrate, ATP, ranged between 150 to 5000 μmol L<sup>-1</sup>, whereas the GDP concentration was fixed at 250, 500, 750, and 1500 μmol L<sup>-1</sup> for both the free enzyme and NME2-ICER. Next, the concentration of the phosphate acceptor, GDP, was varied between 150 and 1000 μmol L<sup>-1</sup>, while the ATP concentration was fixed at 150, 250, 500, and 1000 μmol L<sup>-1</sup> for the free enzyme, and at 150, 500, 750, and 1000 μmol L<sup>-1</sup> for NME2-ICER ATP.

To determine the kinetic parameters  $K_{\text{mapp}}^{\text{ATP}}$  and  $K_{\text{mapp}}^{\text{GDP}}$ , the ATP concentration ranged between 150 to 2000 μmol L<sup>-1</sup>, whilst the GDP concentration was fixed at 1500 μmol L<sup>-1</sup>. Then, the GDP concentration was varied between 150 to



2000  $\mu\text{mol L}^{-1}$ , while the ATP concentration was fixed at 1000  $\mu\text{mol L}^{-1}$ . The kinetic parameters ( $K_{\text{mapp}}^{\text{ATP}}$  and  $K_{\text{mapp}}^{\text{GDP}}$ ) were obtained by nonlinear regression analysis with the aid of the software GraphPad Prism 5.<sup>36</sup>

### Inhibition studies with NME2-ICER

Potential application of the two-dimensional on-flow zonal affinity-based chromatography assay to screen NME2 ligands was verified by using a reference inhibitor, ECG.<sup>37</sup>

The  $\text{IC}_{50}$  for the compound ECG was determined by directly quantifying ADP production in the presence of different concentrations of the inhibitor. First, a positive control for enzymatic activity was obtained in the absence of inhibitor. Reaction mixtures were prepared by mixing 10  $\mu\text{L}$  of GDP stock solution (15  $\text{mmol L}^{-1}$ ), 10  $\mu\text{L}$  of ATP stock solution (50  $\text{mmol L}^{-1}$ ), and 10  $\mu\text{L}$  of ultrapure water. The final volume (100  $\mu\text{L}$ ) was completed with 50  $\text{mmol L}^{-1}$  Tris/HCl buffer, pH 7.0 containing 5  $\text{mmol L}^{-1}$   $\text{MgCl}_2$  and 100  $\text{mmol L}^{-1}$  NaCl. Next, enzymatic activity was measured in the presence of inhibitor. To this end, appropriate ECG stock solutions (ranging from 200 to 3000  $\mu\text{mol L}^{-1}$ ) were prepared in water. Reaction mixtures were prepared by mixing 10  $\mu\text{L}$  of each ECG stock solution with 10  $\mu\text{L}$  of GDP stock solution (15  $\text{mmol L}^{-1}$ ) and 10  $\mu\text{L}$  of ATP stock solution (50  $\text{mmol L}^{-1}$ ). The final volume (100  $\mu\text{L}$ ) was completed with 50  $\text{mmol L}^{-1}$  Tris/HCl, pH 7.0, containing 5  $\text{mmol L}^{-1}$   $\text{MgCl}_2$  and 100  $\text{mmol L}^{-1}$  NaCl.

For each inhibitor concentration, the percentage of inhibition was determined according to equation 2:

$$\text{Inhibition(\%)} = 100 \left[ 1 - \left( \frac{P_i - S_b}{P_0 - S_b} \right) \right] \quad (2)$$

where  $P_i$  is the product (ADP) formed in the presence of inhibitor,  $P_0$  is the ADP product quantified in the absence of inhibitor, and  $S_b$  is ADP quantified during spontaneous ATP hydrolysis.

$S_b$  was determined by injecting the reaction mixture into an empty open tubular silica capillary (blank analysis to quantify spontaneous ATP hydrolysis).

In addition, ECG interference in the ion-pair RP-HPLC separation of the nucleotides was evaluated. For this purpose, an aliquot (20  $\mu\text{L}$ ) of an ECG solution (200  $\mu\text{mol L}^{-1}$ ) in 50  $\text{mmol L}^{-1}$  Tris/HCl buffer, pH 7.0, containing 5  $\text{mmol L}^{-1}$   $\text{MgCl}_2$  and 100  $\text{mmol L}^{-1}$  NaCl was injected into an empty open tubular silica capillary.

The inhibition curve was obtained by plotting the percentage of inhibition *versus* each corresponding ECG concentration, and the  $\text{IC}_{50}$  value was achieved by nonlinear regression analysis with the software GraphPad Prism 5.<sup>36</sup>

## Results and Discussion

### Recombinant NME2 expression and purification

It was used *E. coli* cell strain BL21 (DE3) to overexpress NME2. To evaluate NME2 overexpression levels, we collected aliquots of culture shortly after induction with IPTG. Five hours later, we analyzed them by SDS-PAGE (sodium dodecyl sulfate polyacrylamide gel electrophoresis), which revealed elevated recombinant NME2 levels (Figure 2, lane 2).

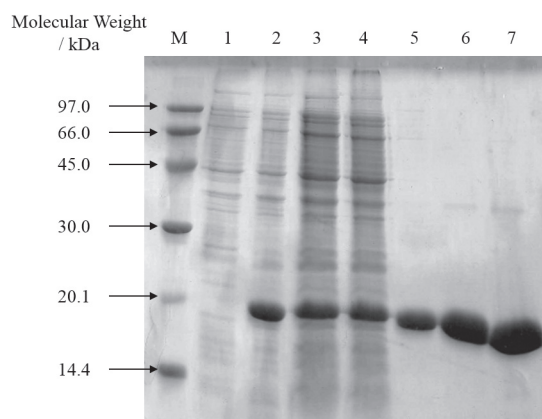


**Figure 2.** SDS-PAGE analysis of NME2 overexpression by *E. coli* strain and NME2 purification by affinity chromatography. The standard protein marker (M) contains phosphorylase b (97 kDa), albumin (66 kDa), ovalbumin (45 kDa), carbonic anhydrase (30 kDa), trypsin inhibitor (20.1 kDa), and  $\alpha$ -lactalbumin (14.4 kDa). Lanes 1 and 2 correspond to whole cell lysate samples before and 5 h after induction with IPTG; lane 3: flow-through sample; lane 4: washing of nonspecific proteins with 40  $\text{mmol L}^{-1}$  imidazole; lanes 5-7: the first three aliquots eluted with 250  $\text{mmol L}^{-1}$  imidazole.

We recovered recombinant NME2 from soluble lysate and purified it on packing Ni-NTA (nitrilotriacetic acid) affinity resin. After that, we washed nonspecific proteins that were weakly bound to the column (Figure 2, lanes 3 and 4) and eluted recombinant NME2 with imidazole gradient (150 to 250  $\text{mmol L}^{-1}$ ). SDS-PAGE showed that the eluted samples presented a single band with molecular mass of approximately 18 kDa, which corresponded to purified recombinant NME2 (Figure 2, lanes 5-7).

### NME2 immobilization

We covalently immobilized NME2 via glutaraldehyde groups on open tubular silica capillary. Immobilization pH greatly influences enzymatic activity, so we investigated immobilization at pH 8.0 and 10.0 for 250  $\text{ng } \mu\text{L}^{-1}$  NME2 in 150  $\text{mmol L}^{-1}$  imidazole buffer containing 300  $\text{mmol L}^{-1}$  NaCl and 50  $\text{mmol L}^{-1}$   $\text{NaH}_2\text{PO}_4$ . We obtained activity recoveries of  $77.9 \pm 2.4\%$  and  $83.3 \pm 0.1\%$  for NME2-ICER

immobilized at pH 8.0 and 10.0, respectively. However, activity of NME2-ICER obtained at pH 10.0 decreased dramatically after 150 days, whereas NME2-ICER obtained at pH 8.0 remained stable for over 300 days. Therefore, we conducted NME2 immobilization at pH 8.0.

The initial activity of six freshly prepared NME2-ICERs from two independent experiments was  $334.6 \pm 37.6 \mu\text{mol L}^{-1}$  (CV = 11.2%,  $n = 6$ ), which demonstrated immobilization procedure repeatability.

### Two-dimensional on-flow zonal affinity-based chromatography assay

We accomplished ion-pair RP-HPLC separation of the nucleotides ATP, ADP, GTP, and GDP, which are involved in the enzymatic reaction, under chromatography conditions previously published by our research group,<sup>28</sup> with modifications. Here, we employed an Eclipse XDB Agilent® (Santa Clara, USA),  $5 \mu\text{m}$  ( $100 \text{ \AA}$ ,  $150 \times 0.46 \text{ mm i.d.}$ ), as analytical column, which reduced analysis time. The nucleotides were separated within 7.5 min in simplified system 2 (Figure 3a). This approach allowed us to follow enzymatic activity by monitoring both products, ADP and GTP. We employed the same chromatography conditions for two-dimensional on-flow zonal affinity-based chromatography assay and system 2 (free NME2 activity assay).

We used two-dimensional on-flow zonal affinity-based chromatography assay to measure NME2-ICER activity. Because flow rate can affect the reaction time between the immobilized enzyme and the substrates, we evaluated flow rates ranging from 30 to  $250 \mu\text{L min}^{-1}$ . Enzymatic activity increased with decreasing flow rate. The highest activity was achieved at  $30 \mu\text{L min}^{-1}$ ; only 30% of the initial activity was recovered at flow rates above  $150 \mu\text{L min}^{-1}$  (Figure 3b). However, the time for total reaction mixture transfer from

NME2-ICER to the analytical column at  $30 \mu\text{L min}^{-1}$  was longer than 5 min. A flow rate of  $100 \mu\text{L min}^{-1}$  best combined high activity (75%) and short transfer time (2.5 min).

Initially, we positioned the valve of the two-dimensional on-flow zonal affinity-based chromatography assay in position A (Figure 1a), which allowed NME2-ICER conditioning in  $50 \text{ mmol L}^{-1}$  Tris/HCl buffer, pH 7.0, and analytical column conditioning in buffer A and methanol (84:16, v/v). After we injected the sample into the system, we switched the valve to position B (Figure 1b) to transfer the compounds of the enzymatic catalysis carried out in NME2-ICER for 2.5 min directly to the analytical column. Next, we switched the valve back to position A. Products and unreacted substrates were separated (7.5 min) in the analytical column. Total analysis time was 10 min (Figure 3a). Table 1 lists event times and chromatographic conditions employed for the two-dimensional on-flow zonal affinity-based chromatography assay.

**Table 1.** Chromatographic conditions of the two-dimensional on-flow zonal affinity-based chromatography assay to evaluate NME2-ICER activity and to screen NME2 ligands

Pump	Valve position	time / min	Event
1	B	0.00-2.50	substrate injection into NME2-ICER and reaction mixture transfer to the analytical column
1	A	2.51-10.0	NME2-ICER conditioning
2	A	2.51-10.0	nucleotide separation and quantification

Pump 1: flow rate =  $100 \mu\text{L min}^{-1}$ , mobile phase =  $50 \text{ mmol L}^{-1}$  Tris/HCl buffer, pH 7.0; pump 2: flow rate =  $1.0 \text{ mL min}^{-1}$ , binary mobile phase = buffer A/methanol (84:16% v/v). Detection at 254 nm. NME2: nucleoside diphosphate kinase B enzyme; ICER: immobilized capillary enzyme reactors.

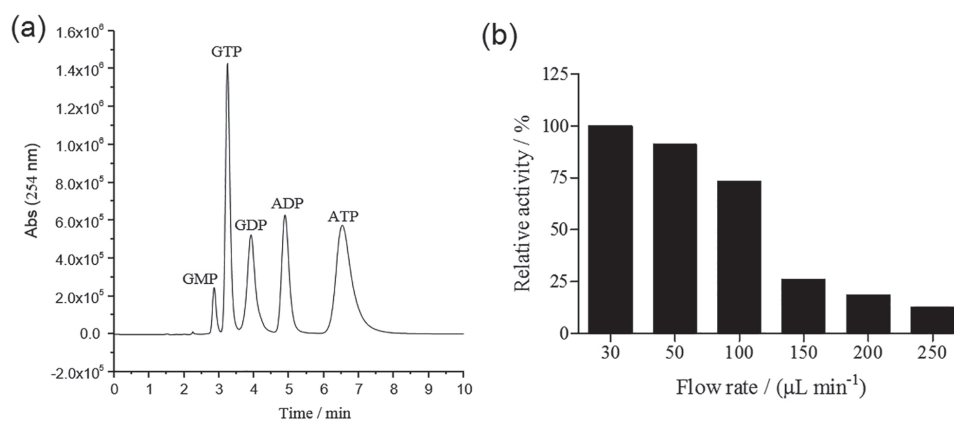


**Figure 3.** (a) Representative chromatogram for the separation of products (GTP and ADP) and unreacted substrates (GDP and ATP) in an ion-pair RP-HPLC column via simplified system 2; (b) relative NME2-ICER activity for different flow rates in system 1 of the two-dimensional on-flow zonal affinity-based chromatography assay. The relative activity was calculated on the basis of the activity obtained at  $30 \mu\text{L min}^{-1}$ , where  $144.9 \mu\text{mol L}^{-1}$  ADP was formed.

### Method qualification

We qualified the two-dimensional on-flow zonal affinity-based chromatography assay and the free NME2 activity assay according to the guidelines for bioanalytical methods.<sup>34</sup> We quantified ADP production by NME2-ICER on the basis of the ADP chromatographic peak area (Figure 3a) at 254 nm. The calibration curve gave a linear relationship for ADP ( $y = 12356x - 187865$ , correlation coefficient ( $r^2$ ) = 0.99) with CV for replicates below 15% and accuracy within 20% of the nominal concentration. LOD and LOQ values were 20 and 100  $\mu\text{mol L}^{-1}$  (CV = 5.3%,  $n = 3$ , accuracy = 10.1%), respectively. When we used the free NME2 activity assay, the calibration curve for ADP was  $y = 11432x + 947100$ ,  $r^2 = 0.99$ , with CV for replicates below 15% and accuracy within 20% of the nominal concentration. LOD and LOQ values were 20 and 50  $\mu\text{mol L}^{-1}$  (CV = 2.8%,  $n = 3$ , accuracy = 1.5%), respectively.

### Enzymatic reaction pH effect

We investigated the enzymatic activity of both free and immobilized enzyme (NME2-ICER) at pH values ranging from 4.0 to 9.0. As illustrated in Figure 4, the pH value influenced free NME2 and immobilized NME2 in similar ways. The enzymes presented relative activity in a wide pH range. Thus, we decided to use an enzymatic reaction pH of 7.0 in further enzyme kinetic and inhibition studies.

### Organic solvent compatibility

Studies have shown that several physicochemical factors may lower enzymatic activity in organic solvents as compared to their activity in water. The presence of organic solvents can influence the enzymatic activity by different mechanisms such as active center blockade,

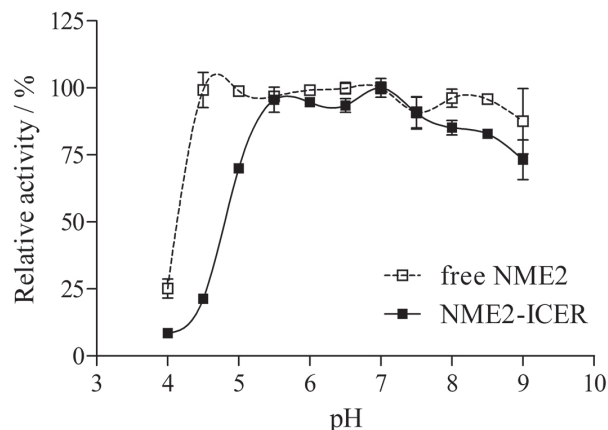


**Figure 4.** Enzymatic reaction pH effect on relative free NME2 and NME2-ICER activities.

unfavorable energy for substrate desolvation (e.g., enzyme-substrate interactions in partially exposed transition states), reduced conformational mobility, suboptimal pH situation, and enzyme and protein denaturation.<sup>38</sup> We assessed two-dimensional on-flow zonal affinity-based chromatography assay compatibility with organic solvent (acetonitrile, DMSO, ethanol, or methanol) in terms of resolution,  $R_s$ , and relative NME2-ICER activity. A minimum resolution of 2.0 is essential for robustness, which results in adequate separation.<sup>35</sup>  $R_s$  was greater than 2.0 only in the presence of methanol and DMSO.

Figure 5 shows that the relative NME2-ICER activity decreased by approximately 20% in the presence of 50% methanol (v/v) or 25% DMSO (v/v) and by 50% in the presence of 50% DMSO (v/v). In the presence of 25% methanol (v/v), the relative activity was totally preserved. Although results revealed that the relative activity was better in the absence of any solvent, NME2-ICER activity could be measured in the presence of methanol or DMSO in the two-dimensional on-flow zonal affinity-based chromatography assay. An important aspect that must be considered in the screening of small molecules is their

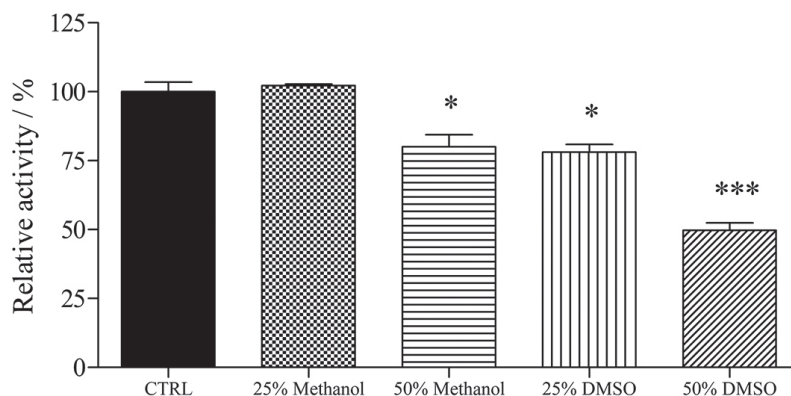


**Figure 5.** Relative NME2-ICER activity in the presence and absence of organic solvents like ethanol and methanol. Different proportions of organic solvents were used in the reaction mixture (25 and 50% v/v) ( $n = 3$ , \*\*\* $p < 0.001$  and \* $p < 0.1$ ).

solubility in organic solvents. The possibility of using organic solvents in our assay is an advantage that allows its application as a ligand screening method.

### Free and immobilized enzyme steady-state kinetics

Free and NME2 reaction steady-state kinetics were evaluated for both free and immobilized NME2. First, four fixed amounts of either ATP or GDP were assayed with increasing concentrations of the other substrate and directly fitted to the Michaelis-Menten equation (Figure 6). These data were then used to construct double-reciprocal plots according to Lineweaver-Burk (Figure 6, insets). When we varied the ATP concentration at a fixed phosphate acceptor (GDP) concentration, we obtained a series of parallel lines in a double reciprocal plot for both free NME2 (Figure 6a, inset) and NME2-ICER (Figure 6b, inset). This pattern is characteristic of a ping-pong mechanism where one product is released before the second substrate combines with the

enzyme.<sup>39,40</sup> We achieved an identical pattern when we varied the GDP concentration at a fixed phosphate donor (ATP) concentration for both free NME2 (Figure 6c, inset) and NME2-ICER (Figure 6d, inset).

Table 2 summarizes apparent  $K_{mapp}$  values estimated from the fit of the data to the Michaelis-Menten equation for both ATP and GDP.

**Table 2.** Kinetics parameters for free and immobilized NME2

Enzyme	$K_{mapp}^{ATP}$ / (mmol L <sup>-1</sup> )	$K_{mapp}^{GDP}$ / (mmol L <sup>-1</sup> )
Free	803.8	832
Immobilized (NME2-ICER)	1136	713

ATP: adenosine 5'-triphosphate di(tris) salt dihydrate; GDP: guanosine 5'-diphosphate sodium salt; NME2: nucleoside diphosphate kinase B enzyme; ICER: immobilized capillary enzyme reactors.

Enzyme immobilization in a support creates a new microenvironment and can affect how the immobilized

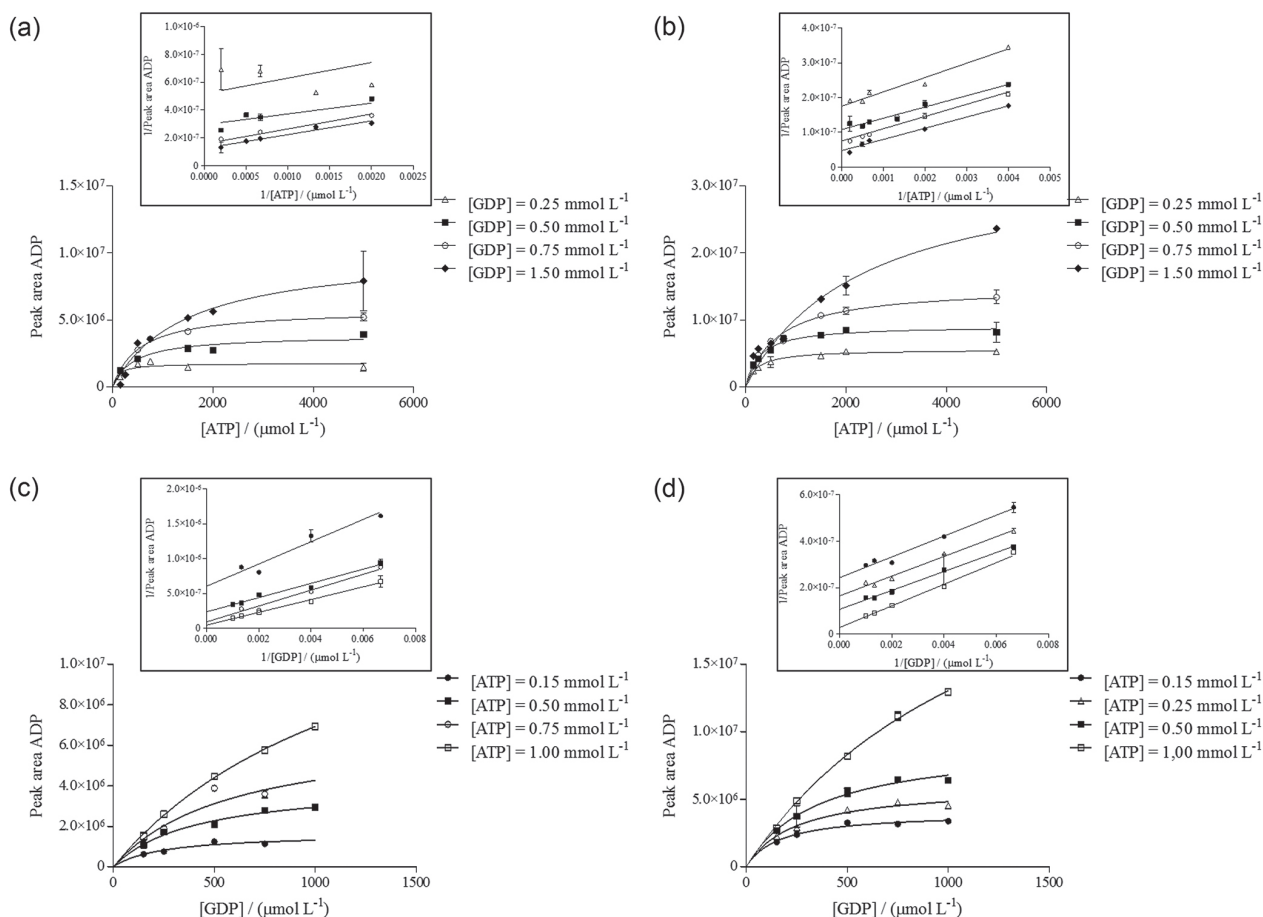


**Figure 6.** Kinetic analysis of enzyme activity of both free enzyme and NME2-ICER. Michaelis-Menten plots when the ATP concentration was varied at fixed GDP concentrations of 0.25 (△), 0.50 (■), 0.75 (○), and 1.50 mmol L<sup>-1</sup> (◆) for NME2-ICER (a) and free NME2 (b). Inset: double-reciprocal plots when the ATP concentration was varied at several fixed GDP concentrations for both NME2-ICER (a) and free enzyme (b). Michaelis-Menten plots when the GDP concentration was varied at several fixed ATP concentrations of 0.15 (●), 0.50 (■), 0.75 (○), and 1.0 mmol L<sup>-1</sup> (□) for NME2-ICER (c) and fixed ATP concentrations of 0.15 (●), 0.25 (△), 0.50 (■) and 1.0 mmol L<sup>-1</sup> (□) for free NME2 (d). Inset: double-reciprocal plots as a function of GDP concentration for both NME2-ICER (c) and free NME2 (d).



enzyme interacts with a substrate. Consequently, some properties of the enzyme molecule, such as catalytic activity, pH, and thermal stability, can change as compared to the free enzyme.<sup>41</sup> However, here we obtained similar results for both free NME2 and NME2-ICER, which showed that the ping-pong catalytic mechanism was preserved, and that free NME2 and NME2-ICER had similar kinetic parameters  $K_{\text{mapp}}^{\text{ATP}}$  and  $K_{\text{mapp}}^{\text{GDP}}$ . Furthermore, substrate inhibition occurred at fixed ATP concentration and higher phosphate acceptor substrate (GDP) levels for both free and immobilized enzymes (data not shown) as previously described for nucleoside diphosphate kinase.<sup>3,42</sup> Hence, NME2 conformational structure and substrate binding sites were minimally altered during NME2 immobilization.

### Inhibition studies

Tea contains polyphenolic compounds such as epigallocatechin gallate (EGCG), epigallocatechin (EGC), and epicatechin gallate (ECG), which suppress cancer cell proliferation. Malmquist *et al.*<sup>37</sup> showed that tea polyphenolic constituents (EGCG, ECG, and flavins) inhibit NME2 activity. To validate the two-dimensional on-flow zonal affinity-based chromatography assay applicability, we used ECG, a well-known NME2 inhibitor.

We determined  $IC_{50}$  for the reference compound ECG by directly quantifying ADP formation. To this end, we measured NME2-ICER activity at fixed and saturating ATP and GDP concentrations and different ECG concentrations. On the basis of Figure 7, ECG had  $IC_{50}$  value of  $161.3 \pm 1.0 \mu\text{mol L}^{-1}$ . Previous studies have demonstrated that ECG is active against free NME2, with an  $IC_{50}$  value of  $170 \mu\text{mol L}^{-1}$ .<sup>37</sup> Although  $IC_{50}$  values for ECG against both free enzyme and NME2-ICER are similar, the  $IC_{50}$  value varies with assay conditions, such as the enzyme and substrate concentrations.<sup>39</sup> NME2-ICER activity decreased after subsequent ECG injection, so we assumed that there was a procedure to recover the activity. However, approximately 20% of the initial NME2-ICER activity was preserved after we injected samples to construct the  $IC_{50}$  curve. Therefore, NME2-ICER recognized ECG as an inhibitor when we employed the two-dimensional on-flow zonal affinity-based chromatography assay. NME2-ICER activity loss due to this inhibitor suggested that the mechanism of NME2 inhibition by ECG was not the traditional reversible mechanism. For this reason, the classic steady state equations for initial velocity cannot be applied to study the ECG mechanism of action against NME2. Clearly, more specific studies, considering ECG slow or tight binding to NME2, must be conducted.

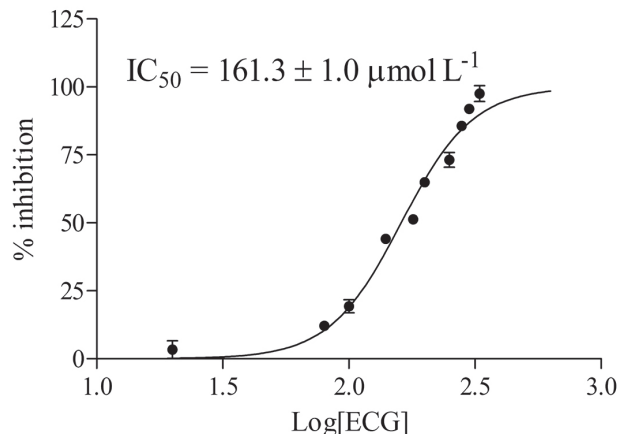


**Figure 7.** Dose-response curve plot of inhibition percentage for NME2-ICER in the presence of epicatechin gallate (ECG).

### Conclusions

The approach described herein represents a significant improvement in the indirect and coupled methods that are usually employed to measure enzyme activity. The strategy reported here is a promising alternative to classic ligand screening methods: two-dimensional on-flow zonal affinity-based chromatography assay using NME2-ICER can be applied in kinetic studies. As demonstrated for the reference inhibitor ECG, the developed assay can be used to identify and to characterize NME2 inhibitors, and it provides the quantitative parameter  $IC_{50}$ . This approach presents several advantages over procedures based on free enzymes in solution, including enzyme reuse for reversible ligands, need for smaller sample amounts, higher analysis speed, and automation.

### Acknowledgments

This work was supported by São Paulo Research Foundation (FAPESP, grant numbers 2013/01710-1, 2014/50249-8). This study was financed in part by Coordenação de Aperfeiçoamento de Pessoal de Nível Superior, Brazil (CAPES), finance code 001, and by the National Council for Technological and Scientific Development (CNPq). J. M. L. and C. S. also acknowledge FAPESP for scholarships (grant numbers 2014/06907-0 and 2014/11640-3). The authors would also like to thank Prof Dr Anita J. Marsaioli for donating the ECG compound.

### References

- de Boer, A. R.; Lingeman, H.; Niessen, W. M. A.; Irth, H.; *TrAC, Trends Anal. Chem.* **2007**, *26*, 867.
- Lascu, I.; Gonin, P.; *J. Bioenerg. Biomembr.* **2000**, *32*, 237.
- Garces, E.; Cleland, W. W.; *Biochemistry* **1969**, *8*, 633.

4. Boissan, M.; Dabernat, S.; Peuchant, E.; Schlattner, U.; Lascu, I.; Lacombe, M.-L.; *Mol. Cell. Biochem.* **2009**, *329*, 51.
5. Lacombe, M. L.; Milon, L.; Munier, A.; Mehus, J. G.; Lambeth, D. O.; *J. Bioenerg. Biomembr.* **2000**, *32*, 247.
6. Steeg, P. S.; Bevilacqua, G.; Kopper, L.; Thorgeirsson, U. P.; Talmadge, J. E.; Liotta, L. A.; Sobel, M. E.; *J. Natl. Cancer Inst.* **1988**, *80*, 200.
7. Anzinger, J.; Malmquist, N. A.; Gould, J.; Buxton, I. L. O.; *Proc. West. Pharmacol. Soc.* **2001**, *44*, 61.
8. Hamby, C. V.; Abbi, R.; Prasad, N.; Stauffer, C.; Thomson, J.; Mendola, C. E.; Sidorov, V.; Backer, J. M.; *Int. J. Cancer* **2000**, *88*, 547.
9. Lee, M.-J.; Xu, D.-Y.; Li, H.; Yu, G.-R.; Leem, S.-H.; Chu, I.-S.; Kim, I.-H.; Kim, D.-G.; *Exp. Mol. Med.* **2012**, *44*, 214.
10. Li, Y.; Tong, Y.; Wong, Y. H.; *Naunyn-Schmiedeberg's Arch. Pharmacol.* **2015**, *388*, 243.
11. Rumjahn, S. M.; Javed, M. A.; Wong, N.; Law, W. E.; Buxton, I. L. O.; *Br. J. Cancer* **2007**, *97*, 1372.
12. Yokdang, N.; Buxton, N. D.; Buxton, I. L. O.; *Proc. West. Pharmacol. Soc.* **2009**, *52*, 88.
13. Tong, Y.; Yung, L. Y.; Wong, Y. H.; *Cancer Lett.* **2015**, *361*, 207.
14. Bouvard, C.; Lim, S. M.; Ludka, J.; Yazdani, N.; Woods, A. K.; Chatterjee, A. K.; Schultz, P. G.; Zhu, S.; *Proc. Natl. Acad. Sci. U. S. A.* **2017**, *114*, 3497.
15. Yokdang, N.; Nordmeier, S.; Speirs, K.; Burkin, H. R.; Buxton, I. L. O.; *Integr. Cancer Sci. Ther.* **2015**, *2*, 192.
16. Wen, S.; Wang, X.; Wang, Y.; Shen, J.; Pu, J.; Liang, H.; Chen, C.; Liu, L.; Dai, P.; *Artif. Cells, Nanomed., Biotechnol.* **2018**, *46*, 896.
17. Parks, R. E. J.; Agarwal, R. P. In *The Enzymes*, vol. 8; Academic Press: New York, 1973, p. 307.
18. Vilela, A. F. L.; da Silva, J. I.; Vieira, L. C. C.; Bernasconi, G. C. R.; Corrêa, A. G.; Cass, Q. B.; Cardoso, C. L.; *J. Chromatogr. B: Anal. Technol. Biomed. Life Sci.* **2014**, *968*, 87.
19. Vanzolini, K. L.; Jiang, Z.; Zhang, X.; Vieira, L. C. C.; Corrêa, G. A.; Cardoso, C. L.; Cass, Q. B.; Moaddel, R.; *Talanta* **2013**, *116*, 647.
20. Vanzolini, K. L.; Vieira, L. C. C.; Corrêa, A. G.; Cardoso, C. L.; Cass, Q. B.; *J. Med. Chem.* **2013**, *56*, 2038.
21. Vilela, A. F. L.; Cardoso, C. L.; *Anal. Methods* **2017**, *9*, 2189.
22. Liang, W.; Hou, Z.; Wang, H.; Xu, W.; Wang, W.; *Chromatographia* **2015**, *78*, 763.
23. Camara, M. A.; Tian, M.; Guo, L.; Yang, L.; *J. Chromatogr. B: Anal. Technol. Biomed. Life Sci.* **2015**, *990*, 174.
24. da Silva, J. I.; de Moraes, M. C.; Vieira, L. C. C.; Corrêa, A. G.; Cass, Q. B.; Cardoso, C. L.; *J. Pharm. Biomed. Anal.* **2013**, *73*, 44.
25. Sobansky, M. R.; Hage, D. S.; *Adv. Med. Biol.* **2012**, *53*, 199.
26. Matsuda, R.; Li, Z.; Zheng, X.; Hage, D. S.; *J. Chromatogr. A* **2015**, *1408*, 133.
27. Vilela, A. F. L.; Seidl, C.; Lima, J. M.; Cardoso, C. L.; *Anal. Biochem.* **2018**, *549*, 53.
28. Lima, J. M.; Vieira, P. S.; de Oliveira, A. H. C.; Cardoso, C. L.; *Analyst* **2016**, *141*, 4733.
29. Slon-Usakiewicz, J. J.; Ng, W.; Foster, J. E.; Dai, J.-R.; Deretey, E.; Toledo-Sherman, L.; Redden, P. R.; Pasternak, A.; Reid, N.; *J. Med. Chem.* **2004**, *47*, 5094.
30. Singh, N.; Ravichandran, S.; Norton, D. D.; Fugmann, S. D.; Moaddel, R.; *Anal. Biochem.* **2013**, *436*, 78.
31. de Moraes, M. C.; Temporini, C.; Calleri, E.; Bruni, G.; Ducati, R. G.; Santos, D. S.; Cardoso, C. L.; Cass, Q. B.; Massolini, G.; *J. Chromatogr. A* **2014**, *1338*, 77.
32. de Oliveira, A. H. C.; Ruiz, J. C.; Cruz, A. K.; Greene, L. J.; Rosa, J. C.; Ward, R. J.; *Protein Expression Purif.* **2006**, *49*, 244.
33. Bradford, M. M.; *Anal. Biochem.* **1976**, *72*, 248.
34. United States Food and Drug Administration (USFDA); *Bioanalytical Method Validation*; USFDA: Rockville, MD. <https://www.fda.gov/media/70858/download>, accessed on August, 2018.
35. Snyder, L. R.; Kirkland, J. J.; Dolan, J. W. In *Introduction to Modern Liquid Chromatography*; Snyder, L. R.; Kirkland, J. J.; Dolan, J. W., eds.; John Wiley & Sons, Inc.: Hoboken, NJ, USA, 2010, p. 19.
36. *GraphPad Prism*, v. 5.0; GraphPad Software Inc., San Diego, CA, USA, 2007.
37. Malmquist, N. A.; Anzinger, J. J.; Hirzel, D.; Buxton, I. L.; *Proc. West. Pharmacol. Soc.* **2001**, *44*, 57.
38. Klivanov, A. M.; *Trends Biotechnol.* **1997**, *15*, 97.
39. Copeland, R. A.; *Evaluation of Enzyme Inhibitors in Drug Discovery*; John Wiley & Sons, Inc.: Hoboken, NJ, USA, 2013.
40. Segel, I. H. In *Encyclopedia of Biological Chemistry*, vol. 2, 2<sup>nd</sup> ed.; Lennardz, W. J.; Lane, M. D., eds.; John Wiley & Sons: New York, 2013, p. 216.
41. Guisán, J. M.; *Immobilization of Enzymes and Cells*, vol. 22, 2<sup>nd</sup> ed.; Human Press: Totowa, NJ, USA, 2006.
42. Schaertl, S.; Konrad, M.; Geeves, M. A.; *J. Biol. Chem.* **1998**, *273*, 5662.

Submitted: January 31, 2019  
Published online: June 7, 2019

